A Fast and Automatic Method for 3D Rigid Registration of MR Images of the Human Brain

Fernanda O. Favretto   Felipe P.G. Bergo   Alexandre X. Falcão

LIV – Institute of Computing – University of Campinas (UNICAMP)

C.P. 6176 – Campinas – SP – 13083-970

{fernandaf,bergo,afalcao}@liv.ic.unicamp.br

Abstract

Image registration is an important problem with several applications in Medical Imaging. Intra-subject rigid registration requires a minimal set of parameters to be computed, and is sufficient for organs with no significant movement or deformation, such as the human brain. Rigid registration has also been used as the first step before inter-subject deformable registration. In this paper we present a fast and automatic method for 3D rigid registration of magnetic resonance images of the human brain. The method combines previous approaches for mid-sagittal plane location and brain segmentation with a greedy-search algorithm to find the best match between source and target images. We evaluated the method on 200 image pairs: 100 without structural abnormalities and 100 with artificially created lesions, such that it was possible to quantify the registration errors. The method achieved very accurate registration within a few seconds.

1. Introduction

Image registration is the process that aligns two or more images in a common reference system of spacial coordinates [12]. This alignment is often done by taking one image domain as reference, transforming corresponding points from each of the other image domains into the reference system, and then extending this transformation to the remaining pixels. The main problems are the choice of suitable point subsets in each image domain and the determination of their mapping functions onto the reference system.

We address both problems in the context of rigid registration between 3D magnetic resonance (MR) images of the human brain, obtained from a same individual in different time instants. Our goal is to register pre- and post-surgical images from epilepsy patients (mostly children), who had lesioned brain tissues removed to eliminate the *foci* of the

seizures. An additional challenge is that, due to tissue removal, some points do not have correspondents in the reference subset. Some patients did not cease the seizures after surgery [27]. Localization and quantification of the variations in the brain tissues for such patients can help neurologists to understand the phenomenon and develop new treatments.

We propose a fast and automatic method for 3D rigid registration, where the point subsets are obtained from the surface of the brain through segmentation [2] and their correspondence is found in two steps. The first step aligns the images by the mid-sagittal plane (MSP) [3] and the second step completes registration by using a greedy-search algorithm to find the mapping function between the source (reference) and target point subsets. Indeed, the MSP location already uses the brain segmentation proposed in [2], so we are also taking advantage of a subproduct of the MSP location approach for registration.

The literature of medical image registration is vast, but our method presents several desirable characteristics simultaneously, which make of it an important contribution: It is fully 3D, simple, fast, and automatic. It has been extensively evaluated on 3D MR-T1 images of the human brain, with very accurate results. The experiments involved 200 target images, 100 without structural abnormalities and 100 with artificially created lesions, such that it was possible to quantify the registration errors.

This paper is organized as follows. Section 2 presents a short review on medical image registration. The proposed method is described in Section 3 and the experiments with discussion are presented in Section 4. Finally, we state conclusions and future work in Section 5.

2. Related Works

Medical image registration has been useful to combine data from the same and different imaging modalities, such that it becomes possible to visualize changes in anatomy and physiology along time and under different conditions,

and to assist image-guided surgery, radiotherapy, and other treatments. The literature is vast and there are several books and surveys about medical image registration methods [12, 5, 1, 13, 20, 29, 16].

In [20], the authors classify registration methods according to the nature of the registration basis, nature of the transformation, domain of the transformation, user-interaction level, transformation search method, image modality, and transformation subject. These seven criteria are further subdivided in some levels as follows. According to the nature of the registration basis, a method can be further classified as *object-based* or *image-based*. Object-based methods are those that consider image segmentation (objects, points, lines) to find the transformation [11, 4], while image-based methods avoid segmentation for registration [6, 21, 19]. The nature of the transformation can be *rigid* or *deformable*. Rigid registration methods allow only rotations and translations, while deformable registration methods may change the shape and form of the structures in the image. Methods can also be classified according to the domain of the transformation as *global* or *local*. In global approaches, a same transformation is applied to the whole image domain. When different parts of the image have distinct transformations, the method is said local. According to the user-interaction level, we classify the methods in *interactive* and *automatic* approaches. Interactive methods require user intervention in one or more registration steps, such as for point selection or segmentation, point correspondence, and adjustment of the registration parameters [15]. Otherwise, the user only provides the input images and the method is said automatic [18]. In [20], a distinction is made between interactive and semi-automatic. There, interactive means manual registration — the user provides the transformation. Their concept of semi-automatic is what we call interactive. Therefore, interactive to us stands for manual and semi-automatic registrations. The transformation search further divides the methods in those based on *parameter estimation* and *parameter search*. The former estimates the registration parameters from given point correspondences and the latter determine the parameters by finding an optimum of some function defined in the parameter space [23, 25]. The methods can also be called *mono-modal* or *multi-modal*, depending on the imaging modalities of the source and target images being the same or not. Finally, if the images are from a same subject, the methods are called *intra-subject*, and *inter-subject* otherwise [7, 8, 11].

According to the above criteria, our registration method is classified as object-based, since the brain is segmented to define the point subsets for registration; rigid, mono-modal and intra-subject, since we are interested in aligning MR images from a same patient; global, since the transformation for the point subsets is the same for the rest of the image domain; automatic, given that the user only provides the input images; and based on parameter search.

Due to the size of the literature and the lack of detailed information in most papers, it is impossible to affirm that our method is the best option for rigid registration of MR-T1 images. However, we have observed in recent works that several approaches are not efficient for 3D images or have only been demonstrated for 2D images [30, 26, 17, 28], are not automatic [22, 15], have often been presented with no quantitative evaluation [15, 24, 9, 30], and seem to be limited to some applications [18, 14]. Our method is fully 3D, fast, simple, automatic, and has been extensively evaluated with abnormal images. Currently, it is limited to MR-T1 images, since the algorithms used for image alignment [3] and segmentation [2] are modality-specific, but the main idea can be used with other methods which are independent of imaging modality.

A recent approach [18], for instance, uses a similar strategy for 3D rigid registration of MR-T1 images. Instead of pre-aligning images by the mid-sagittal plane (MSP), it estimates the equivalent meridian plane (EMP), which contains the first and second principal axes computed by principal component analysis (PCA). The process is then completed by searching for the transformation within a small neighborhood, using Powell's approach [23] and maximal mutual information as optimization criterion. The authors claim 100% acceptable registrations with a mean execution time of 221 seconds (3.69 minutes, P4 3.0 GHz). However, brain alterations due to brain asymmetries can modify the EMP location and cause failure in registration. MSP location [3], using the corresponding brain segmentation [2], has been successfully evaluated for patients with lesions and surgical cavities.

Another recent approach for registration of MR images of the brain addresses a similar problem, where the matching is partial between source and target images [14]. It uses a probabilistic search algorithm over the parameter space in order to find a rigid transformation. Initially, the entire space is divided into a number of candidate parameter sets with uniform distribution. The results of rigid registration for each set are used to rank another number of the best candidate parameter sets with normal distribution. The authors claim that the method converges to the optimal rigid registration in a finite number of iterations, and they further refine registration using a deformable approach. The authors evaluated the 2D case, where their method took from 57 to 101 seconds to register a single 2D slice to a 3D volume (Athlon 2.2 GHz).

3. Method

A 3D MR image $\hat{I}$ is a pair (D_I, I), where $D_I \subset Z^3$ is the image domain and $I(v)$ is the intensity of a voxel $v = (x, y, z) \in D_I$. Let $\hat{I} = (D_I, I)$ and $\hat{J} = (D_J, J)$

be the source (reference) and the target images of the brain for registration. The point subsets in D_I and D_J are defined as S_I and S_J, respectively. We assume that $\hat{I}$ and $\hat{J}$ are aligned by the mid-sagittal plane (MSP), using the approach proposed in [3], which in turn segments the brain by automatic tree pruning [2] (Sections 3.1– 3.3). These methods have been designed for MR-T1 images, but any other approach to align images based on the MSP and to segment the brain can be used to extend our method to other modalities. We provide two options to define the subsets S_I and S_J from the surface of the brain and provide a greedy-search algorithm to find the transformation $T(S_J) \approx S_I$ that maps S_J into their correspondent points in S_I. This last step is described in Section 3.4, and the registration process completes by applying T to the remaining voxels of D_J.

3.1. Automatic Brain Segmentation

Some steps of our method requires the segmentation of the brain. We use the automatic tree pruning, a graph-based segmentation approach that is fast, does not rely on templates and performs well regardless of age and anatomic variations [2]. It employs automated histogram analysis and mathematical morphology to select a set of markers inside the brain. An optimum path forest [10] is computed from these markers, and the tree pruning technique evaluates the forest automatically to detect the edges that cross the object's border, and then prunes the subtrees at these edges. The resulting forest is a reasonable segmentation of the brain. This method takes about 55 seconds to compute the segmentation of a typical MR volume [2, 3], using a 2.0 GHz desktop PC. Figure 1 shows sample results from this segmentation technique.

3.2. MSP Location

We use the MSP location method described in [3]. The MSP matches the longitudinal fissure that separates the brain hemispheres, which is filled with cerebro-spinal fluid (CSF). In MR-T1, CSF appears as low intensity voxels. The method requires brain segmentation, and locates an initial MSP candidate aligned with the sagittal plane of the acquisition. The mean intensity of the voxels in the intersection of the candidate plane with a brain segmentation mask is used as score. From the initial MSP candidate, the method performs a greedy heuristic search that minimizes the score. Given a brain segmentation (which can be computed as per Section 3.1), this method takes about 5 seconds to locate the MSP in a typical MR volume, using a 2.0 GHz desktop PC, and is applicable to children and patients with structural abnormalities, such as lesions and surgical cavities. Figure 2 shows examples of MSPs located by this method in patients with large surgical cavities.
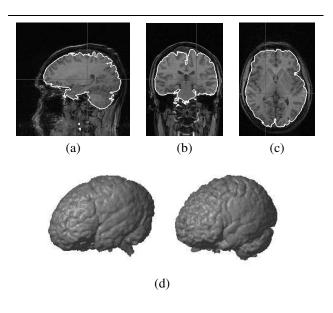

(a)   (b)   (c)

(d)

Figure 1. Automatic brain segmentation by tree pruning: (a), (b), (c): object borders on sample 2D slices. (d): 3D rendition of the brain object.

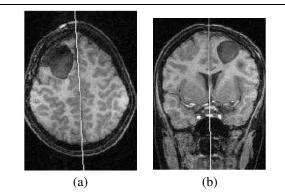(a)   (b)

Figure 2. Computed MSPs in MR images of patients with large surgical cavities.

3.3. Image alignment based on MSP

After the MSP has been located in each of the input images, we apply a transformation to reformat the images such that their MSP (xy-plane) will be located at a same coordinate along the z-axis. In this reference system, the new images $\hat{I}$ and $\hat{J}$ must be registered as described next.

3.4. Greedy Transformation Search

For given point sets $S_I \subset D_I$ and $S_J \subset D_J$, already aligned by the MSP, let $\hat{I}_s = (S_I, I)$ and $\hat{J}_s = (S_J, J)$ be the respective subimages of $\hat{I}$ and $\hat{J}$. We need to search only for a rigid transformation T, which performs rotation θ_z around the z-axis and translations t_x and t_y along x and y axes. Considering all possible combinations of $\theta_z \in \{0°, \pm0.5°, \pm1°, \pm5°\}$ rotations and $t_x, t_y \in \{0mm, \pm1mm, \pm5mm\}$ translations, we define a basis Φ_i, $i = 1, 2, \ldots, n$, of $n = 175$ transformations. The optimum transformation T is computed as a sequence of transformations Φ_i, which produces strictly decreasing matching errors.

We have evaluated S_I and S_J as the voxels on the respective brain surfaces, called *border sets*, and as the voxels within a 3D band of $3mm$ around the brain surfaces, called *band sets*. For a given T, a subimage $\hat{J}'_s = (S'_J, J)$ is created by applying $T(S_J) = S'_J$, and the registration error is measured by a distance/similarity function $D(\hat{I}_s, \hat{J}'_s)$. We define the following measures for evaluation: D_1 – the total absolute error between voxel coordinates, D_2 – the total square error between gradient values, D_3 – the mutual information based on the voxel intensities and D_4 – the mutual information based on the voxel gradient values. The distance functions D_1 and D_2 are minimized for registration, while the similarity functions D_3 and D_4 are maximized. We label the evaluated possibilities $M1 \ldots M4$, as shown in Table 1.

More formally, let $\delta(u - v) = 1$ if $u = v$ for $u \in S_I$ and $v \in S'_J$, and $\delta(u - v) = 0$ otherwise. Consider also the complementary function $\bar{\delta}(u - v) = 1 - \delta(u - v)$. Let $x_1 = I(u)$ and $x_2 = J(v)$ be the intensities of voxels $u \in S_I$ and $v \in S'_J$, respectively. The probability density functions $p(x_1)$ and $p(x_2)$, and the joint probability density function $p(x_1, x_2)$ are computed as follows.

$$p(x_1) = \sum_{\forall u \in S_I} \frac{\delta(I(u) - x_1)}{|S_I|} \tag{1}$$

$$p(x_2) = \sum_{\forall v \in S_J} \frac{\delta(J(v) - x_2)}{|S_J|} \tag{2}$$

$$\begin{aligned} p(x_1, x_2) = &\frac{1}{|S'_J|} \sum_{\forall u \in S_I, v \in S'_J} \\ &\delta(u - v)\delta(I(u) - x_1)\delta(J(v) - x_2) \\ + &\bar{\delta}(u - v)\delta(K - x_1)\delta(J(v) - x_2) \end{aligned} \tag{3}$$

where K is the maximum value of $\hat{I}_s$ plus one. This second part of Equation 3 is used to penalize the mismatching between S_I and S'_J in the computation of the mutual information $M(\hat{I}_s, \hat{J}'_s)$.

$$M(\hat{I}_s, \hat{J}'_s) = \sum_{\forall(x_1, x_2)} p(x_1, x_2) \log \frac{p(x_1, x_2)}{p(x_1)p(x_2)} \tag{4}$$

Similarly, we compute the morphological gradients $\hat{G} = (D_I, G)$ and $\hat{H} = (D_J, H)$ of both images, $\hat{G}_s = (S_I, G)$, $\hat{H}_s = (S_J, H)$, $\hat{H}'_s = (S'_J, H)$, and finally, the mutual information $M(\hat{G}_s, \hat{H}'_s)$. Therefore, the above measures are:

$$D_1(S_I, S'_J) = \sum_{\forall u \in S_I, v \in S'_J} \bar{\delta}(u - v) \tag{5}$$

$$\begin{aligned} D_2(\hat{G}_s, \hat{H}'_s) = &\sum_{\forall u \in S_I, v \in S'_J} \delta(u - v)(G(u) - H(v))^2 \\ &+ \bar{\delta}(u - v)(L - H(v))^2 \end{aligned} \tag{6}$$

$$D_3(\hat{I}_s, \hat{J}'_s) = M(\hat{I}_s, \hat{J}'_s) \tag{7}$$

$$D_4(\hat{G}_s, \hat{H}'_s) = M(\hat{G}_s, \hat{H}'_s) \tag{8}$$

where L is the maximum gradient value in $\hat{G}_s$ plus 1. Algorithm 1 presents the proposed greedy search to find the transformation T which minimizes a distance measure $D(\hat{I}_s, \hat{J}'_s)$. It is not difficult to modify it to either minimize/maximize any of the measures D_i, $i = 1, 2, 3, 4$, above.

Algorithm 1 GREEDY TRANSFORMATION SEARCH

INPUT: Images $\hat{I}_s = (S_I, I)$ and $\hat{J}_s = (S_J, J)$, distance function D, transformation basis Φ_i, $i = 1, 2, \ldots n$.

OUTPUT: The best transformation T.

1.   Set $T = \mathbf{I}$ and $D_{\min} \leftarrow D(\hat{I}_s, \hat{J}_s)$.
2.   **Repeat**
3.   Set $k \leftarrow nil$.
4.   **For** $i = 1$ **to** n **do**
5.   Set $T' \leftarrow T \times \Phi_i$ and $\hat{J}'_s \leftarrow (T'(S_J), J)$.
6.   Set $d \leftarrow D(\hat{I}_s, \hat{J}'_s)$.
7.   **If** $d < D_{\min}$ **then**
8.   Set $D_{\min} \leftarrow d$, $k \leftarrow i$.
9.   **If** $k \neq nil$ **then** Set $T \leftarrow T \times \Phi_k$.
10.   **Until** $k = nil$.
11. **Return** T.

Clearly, the above algorithm does not guarantee the global optimum. However, as we will see, it has produced very accurate results in all evaluated cases. Starting from the identity transformation $T = \mathbf{I}$, which produces a distance $D_{\min} = D(\hat{I}_s, \hat{J}_s)$ (Line 1), each iteration of the algorithm looks for the next local transformation Φ_k, $1 \leq k \leq n$, which minimizes $D_{\min}$ among all possible cumulative transformations $T \times \Phi_i$, $i = 1, 2, \ldots, n$ (Lines 2–10). By these local minimization steps, we expect to converge to the desired minimum after a finite number of iterations. Indeed, it is guaranteed that the algorithm will finish because it computes a sequence of cumulative transformations with strictly decreasing distances.

We have evaluated the algorithm over border and band sets according to Table 1. These sets are obtained from the surface of a segmented brain, as the one shown in Figure 1.

Method	Set	Measure	Image Feature
M1	Border	Total absolute error (Eq. 5)	Voxel coordinates
M2	Band	Total square error (Eq. 6)	Voxel gradient intensities
M3	Band	Mutual information (Eq. 7)	Voxel intensities
M4	Band	Mutual information (Eq. 8)	Voxel gradient intensities

Table 1. Point subsets, distance/similarity measures and image features evaluated.

The border set with the voxels of the brain surface and the band set with the voxels within a $3mm$ band around the brain surface. The basic difference between them is illustrated in Figure 3.
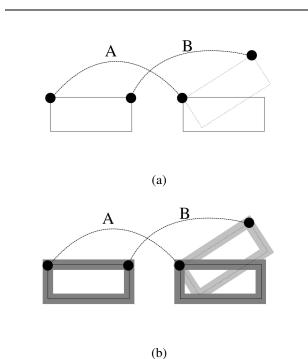

(a)

(b)

Figure 3. (a) Match A and mismatch B between border pixels. (b) Match A and mismatch B between band pixels.

3.5. Visualization

The transformation T computed by Algorithm 1 is then applied to the entire target image domain. We compose a visualization that alternates the source and registered target in a checkerboard pattern, allowing the user to inspect the registration for correctness, coherence and continuity. Figure 4 shows examples of this visualization with a registration obtained with the proposed method.

4. Experimental Results

We performed tests with two sets of images. In the first set, the source and target images differ only by a known rigid transformation (rotations and translations). In the second set, we created synthetic lesions in the target images, and then applied known rigid transformations to them.

Both sets were based on 20 MR-T1 volumes of the brain, each acquired with a voxel size of $0.98 \times 0.98 \times 1.00mm^3$. All volumes were interpolated to an isotropic voxel size of $0.98mm^3$. After applying the MSP location method, all images were reformatted to align the MSP to the sagittal plane of the reference coordinate system.

For each aligned source image, we generated 5 transformed targets, by applying known compositions of random translations ($-20mm \leq t_x, t_y \leq 20mm$) and random rotations ($-20° \leq \theta_z \leq 20°$). Therefore, we had 100 source-target image pairs in the first set.

In the second set, for each source image we created 5 target images by adding random rigid transformations and synthetic lesions, using the *Phantom Lesion* filter in the IVS software [1]. Therefore, this set also had 100 source-target image pairs. Figure 5 shows an example of synthetic lesion.

In the first experiment, we performed registrations of the 100 image pairs in set 1 (no lesions) using the 4 methods $M1 \ldots M4$ of Table 1. We computed the mean error and standard deviation of the error for each parameter. We also measured the mean time required to perform the search with Algorithm 1 running on an Athlon64 X2 3800+ (2.0 GHz). Table 2 shows the results.

The registration method is quite accurate for rigid registration of MR images of the brain with no lesions. The same evaluation was performed on the 100 image pairs in set 2 (with synthetic lesions). The results for this set are shown in Table 3.

The registration error is not significantly affected by the presence of the synthetic lesions. These results show that the proposed method can be applied for rigid registration of MR images of the brain even in the presence of lesions. Figure 4 shows slices from an image pair in this set. In that particular example the translation error was about 1 voxel (0.98 mm).

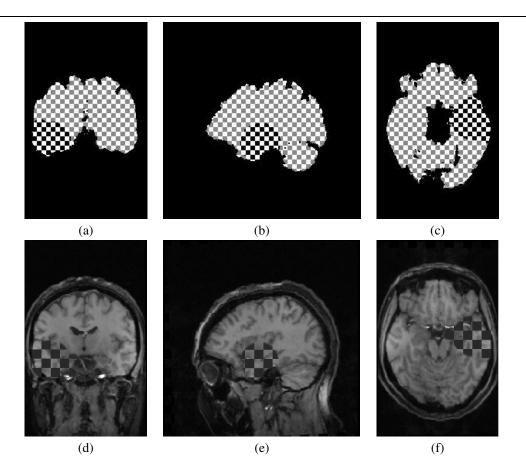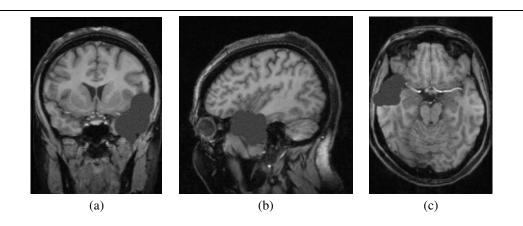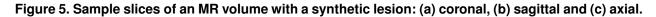1 http://www.liv.ic.unicamp.br/~bergo/ivs

Figure 4. Checkerboard display of source and registered (target) brain masks: (a) coronal view, (b) sagittal view, and (c) axial view. White squares come from the target and gray squares come from the source. This target has a synthetic lesion not present in the source image. (d), (e), (f): checkerboard display of source and target MR images. The visible squares represent the lesion.

Figure 5. Sample slices of an MR volume with a synthetic lesion: (a) coronal, (b) sagittal and (c) axial.

Method	R_Z Mean Error	T_X Mean Error	T_Y Mean Error	Search Time
$M1$	0.12 ° ($\sigma = 0.21$)	1.00 mm ($\sigma = 0.86$)	0.85 mm ($\sigma = 0.85$)	19 s
$M2$	0.13 ° ($\sigma = 0.22$)	1.06 mm ($\sigma = 0.86$)	0.93 mm ($\sigma = 0.86$)	117 s
$M3$	0.09 ° ($\sigma = 0.20$)	1.19 mm ($\sigma = 0.74$)	1.04 mm ($\sigma = 0.85$)	358 s
$M4$	0.15 ° ($\sigma = 0.23$)	0.41 mm ($\sigma = 0.62$)	0.71 mm ($\sigma = 0.77$)	359 s

Table 2. Evaluation of the registration method on the first image set (100 image pairs, no lesions): Mean error (with standard deviations σ) for the 3 registration parameters and mean search time.

Method	R_Z Mean Error	T_X Mean Error	T_Y Mean Error	Search Time
$M1$	0.17 ° ($\sigma = 0.28$)	1.09 mm ($\sigma = 0.96$)	0.96 mm ($\sigma = 0.98$)	23 s
$M2$	0.12 ° ($\sigma = 0.21$)	0.91 mm ($\sigma = 0.93$)	0.80 mm ($\sigma = 0.83$)	105 s
$M3$	0.20 ° ($\sigma = 0.36$)	1.26 mm ($\sigma = 0.62$)	1.26 mm ($\sigma = 1.01$)	341 s
$M4$	0.19 ° ($\sigma = 0.36$)	1.38 mm ($\sigma = 0.92$)	1.33 mm ($\sigma = 1.34$)	324 s

Table 3. Evaluation of the registration method on the second image set (100 pairs, with synthetic lesions): Mean error (with standard deviations σ) for the 3 registration parameters and mean search time.

It is important to note that $M1$ is the simplest and fastest method in our registration approach. The results with $M1$ do not present significant differences in accuracy with respect to $M2 \ldots M4$.

5. Conclusions and Future Work

Image registration is an important task that enables comparative analysis of images acquired at different occasions (different modalities, before and after a significant clinical event such as a surgery, or for comparison between distinct individuals in a population) [12]. Rigid registration is simple and directly applicable to organs without significant shape change, such as the human brain.

We presented a simple and fast rigid registration method that can be applied to 3D MR images of the brain. It is based on automatic brain segmentation [2], automatic mid-sagittal plane location [3], image alignment, and a greedy transformation search. Our method performs 3D-3D registration in under 90 seconds for typical brain MR volumes with 1-mm^3 voxels. Most of this time (60 seconds) is used for the preprocessing (brain segmentation and MSP location), while the registration itself takes about 20 seconds. This is a considerable speed improvement over recent works that require about 220 seconds for 3D-3D registration [18] and up to 100 seconds for a single 2D-3D registration [14].

As future work, we intend to test the method in clinical data with actual lesions (pre- and post-surgical images).

References

[1] M. Audette, F. Ferrie, and T. Peters. An algorithmic overview of surface registration techniques for medical imaging. *Medical Image Analysis*, 4(3):201–217, 2000.

[2] F. P. G. Bergo, A. X. Falcão, P. A. V. Miranda, and L. M. Rocha. Automatic image segmentation by tree pruning. *J Math Imaging and Vision*, 29(2–3):141–162, Nov 2007.

[3] F. P. G. Bergo, G. C. S. Ruppert, L. F. Pinto, and A. X. Falcão. Fast and robust mid-sagittal plane location in 3D MR images of the brain. In *Proc. BIOSIGNALS 2008 – Intl. Conf. on Bio-Inspired Syst. and Sig. Proc.*, pages 92–99, Jan 2008.

[4] P. J. Besl and N. D. McKay. A method for registration of 3-d shapes. *IEEE Transactions on pattern analysis and machine intelligence*, 14(2):239–256, 1992.

[5] L. G. Brown. A survey of image registration techniques. *ACM. Computing Surveys*, 24:326–376, 1992.

[6] E. D. Castro and C. Morandi. Registration of translated an rotated images using finite fourier transforms. *IEEE Transactions on Pattern Analysis and Machine Intelligence*, PAMI-9(5):700–703, 1987.

[7] D. L. Collins, A. C. Holmes, and T. M. Peters. Automatic 3d segmentation of neuro-anatomical structures from mri. *Information processing in medical imaging*, pages 139–152, 1995.

[8] D. L. Collins, P. Neelin, T. M. Peters, and A. C. Evans. Automatic 3d intersubject registration of mr volumetric data in

standardized talairach space. *Journal of computer assisted tomography*, 18(2):192–205, 1994.

[9] A. Dhawan, L. K. Arata, A. V. Levy, and J. Mantil. Iterative principal axes registration method for analysis of mr-pet brain images. *Biomedical Engineering, IEEE Transactions on*, 42:1079 – 1087, Nov 1995.

[10] A. X. Falcão, J. Stolfi, and R. A. Lotufo. The image foresting transform: Theory, algorithms and applications. *IEEE Trans. on Pattern Analysis and Machine Intelligence*, 26(1):19–29, Jan 2004.

[11] J. Feldmar, G. Malandain, J. Declerck, and N. Ayache. Extension of the icp algorithm to non-rigid intensity-based registration of 3d volumes. In *Mathematical methods in biomedical image analysis*, pages 84–93. IEEE computer society press, Los Alamitos, CA, 1996.

[12] J. Hajnal, D. L. G. Hill, and D. J. Hawkes. *Medical Image Registration*. CRC Press, London, 2001.

[13] L. Hallpike and D. J. Hawkes. Medical image registration: an overview. *Imaging*, 14(6):455–463, Dec 2002.

[14] J. Han, M. Qiao, J. Hornegger, T. Kuwert, W. Bautz, and W. Romer. Automatic sub-volume registration by probabilistic random search. *Medical Imaging - Image Processing - Proceedings of SPIE*, 6144:799–807, 2006.

[15] C. Huang, C. Jiang, and W. Sung. Medical image registration and fusion with 3d ct and mr data of head. *Computer-Based Medical Systems*, pages 401 – 404, 2006.

[16] P. J. Kostelec and S. Periaswamy. Image registration for mri. *Modern Signal Processing*, 46:161–184, 2003.

[17] C. Liu, K. Li, and Z. Liu. Medical image registration by maximization of combined mutual information and edge correlative deviation. *Engineering in Medicine and Biology Society*, pages 6379 – 6382, 2005.

[18] Z. Lu, Q. Feng, P. Shi, and W. Chen. A fast 3-D medical image registration algorithm based on equivalent meridian plane. *Image Processing*, 5:357–360, 2007.

[19] F. Maes, A. Collignon, D. Dandeermeulen, G. Marchal, and P. Suetens. Multimodality image registration by maximization of mutual information. *IEEE Transactions in Medical Imaging*, 16:187–198, 1997.

[20] J. B. A. Maintz and M. A. Viergever. A survey of medical image registration. *Medical Image Analysis*, 2(1):1–36, 1998.

[21] W. M. W. I. P. Viola. Alignment by maximization of mutual information. *International Journal of Computer Vision*, 24(2):137–154, Sep 1995.

[22] U. Pietrzyk, K. Herholz, G. Fink, A. Jacobs, R. Mielke, I. Slansky, M. Wurker, and W.-D. Heiss. An interactive technique for three-dimensional image registration: validation for PET, SPECT, MRI and CT brain studies. *Journal of Nuclear Medicine*, 35(12):2011–2018, 1994.

[23] M. J. D. Powell. An efficient method for finding the minimum of a function of several variables without calculating derivatives. *Computer Journal*, 7:155–162, 1964.

[24] R. J. Tait, G. Schaefer, A. A. Hopgood, and S. Y. Zhu. Efficient 3-d medical image registration using a distributed blackboard architecture. *Engineering in Medicine and Biology Society*, 3:3045 – 3048, Sep 2006.

[25] D. Vandermeulen, F. Maes, and P. Suetens. Comparative evaluation of multiresolution optimization strategies for multimodality image registration by maximization of mutual information. *Medical Image Analysis*, 3(4):373–386, 1999.

[26] H. H. Wen, W. C. Lin, and C. T. Chen. Knowledge-based medical image registration. *Engineering in Medicine and Biology Society*, 3:1200 – 1201, Nov 1996.

[27] C. L. Yasuda, C. C. Valise, A. V. Saúde, A. L. F. Costa, F. R. Pereira, M. Morita, L. E. Betting, H. Tedeschi, E. Oliveira, G. Castellano, and F. Cendes. Recovery of white matter atrophy (WMA) after successful surgery in mesial TLE. In *Proc. 60th Annual Meeting of the American Academy of Neurology*, page to appear, 2008.

[28] H. Zhou, T. Liu, F. Lin, Y. Pang, J. Wu, and J. Wu. Towards efficient registration of medical images. *Computerized Medical Imaging and Graphics*, 31:374 – 382, Sep 2007.

[29] B. Zivota and J. Flusser. Image registration methods: a survey. *Image and Vision Computing*, 21:977–1000, 2003.

[30] X. Zou, X. Zhao, and Y. Feng. An efficient medical image registration algorithm based on gradient descent. *Complex Medical Engineering*, pages 636 – 639, May 2007.